SCIENCE CHINA
Chemistry

• REVIEWS •
• SPECIAL TOPIC • Fluorescent Chemical/Biological Sensors and Imaging

January 2016 Vol.59 No.1: 16–29
doi: 10.1007/s11426-015-5504-9

SERS-based mercury ion detections: principles, strategies and recent advances

Chunyuan Song, Boyue Yang, Yanjun Yang & Lianhui Wang*

Key Laboratory for Organic Electronics & Information Displays; Institute of Advanced Materials, Jiangsu National Synergetic Innovation Center for Advanced Materials, Nanjing University of Posts & Telecommunications, Nanjing 210023, China

Received June 30, 2015; accepted August 17, 2015; published online December 10, 2015

Mercury ion (Hg^{2+}), known as one of the highly toxic and soluble heavy metal ions, is causing serious environmental pollution and irreversible damage to the health. It is urgent to develop some rapid and ultrasensitive methods for detecting trace mercury ions in the environment especially drink water. Surface-enhanced Raman scattering (SERS) is considered as a novel and powerful optical analysis technique since it has the significant advantages of ultra-sensitivity and high specificity. In recent years, the SERS technique and its application in the detection of Hg^{2+} have become more prevalent and compelling. This review provides an overall survey of the development of SERS-based Hg^{2+} detections and presents a summary relating to the basic principles, detection strategies, recent advances and current challenges of SERS for Hg^{2+} detections.

mercury ion, surface-enhanced Raman scattering, detection strategy, turn-on, turn-off

Citation: Song CY, Yang BY, Yang YJ, Wang LH. SERS-based mercury ion detections: principles, strategies and recent advances. *Sci China Chem*, 2016, 59: 16–29, doi: 10.1007/s11426-015-5504-9

1 Introduction

Mercury, one of the most toxic heavy metals, exists widely in the nature. Soluble inorganic mercury is considered as the main source of mercury pollution, which is released into the environment from both natural sources including volcanic and ocean emissions, and anthropogenic sources such as coal and gold mining, chemical manufacturing, solid waste incineration as well as pigment's and dental amalgams [1,2]. Currently, inorganic mercury slips into the nature water through direct wastewater discharge and global mercury cycle via atmospheric circulation and precipitation. The contaminated water with water-soluble mercuric ions (Hg^{2+}) has become one of the major harms of human health. In waters, some bacteria which reside in aquatic sediments and fishes can convert Hg^{2+} into methylmercury which is known as a potent neurotoxin that is readily absorbed but poorly discharged by the body. Once inorganic mercury including methylmercury enters the food chain, it will accumulate in animals and plants, and then biomagnify in higher organisms and subsequently be ingested by humans [3]. Gradually, excessive accumulation of mercury in human body causes permanent brain damage with serious clinical symptoms such as headache, forgetfulness, deafness, visual impairment and cognitive disorders [1,4]. Even more alarming is that if exposed to toxic levels of mercury babies are likely to have different degrees of mental retardation, autism, paralysis and even death [5,6]. For human health, the United States Environmental Protection Agency (EPA) has enacted a maximum residue limit in drinking water as 10 nmol/L for Hg^{2+} [7]. Thus, it is very urgent to develop rapid, sensitive and selective methods for detecting Hg^{2+}.

Currently, various analytic methods for mercury ions in water have been developed. Some of them are rapid and

*Corresponding author (email: iamlhwang@njupt.edu.cn)

accurate, such as electrothermal atomic absorption spectrometry (ETAAS) [8,9], enzyme-linked immunosorbent assay (ELISA) [10], hydride generation atomic absorption spectrometry (HGAAS) [11] and cold vapor atomic fluorescence spectrometry (CA-AFS) [12]. However, these technologies usually require complex and expensive apparatuses or complicated sample preparation processes, which make them not suitable for *in-situ* analysis. Other methods such as colorimetry, resonance scattering spectral assay, electrochemistry and fluorescence [7,10,13–17] have lower requirements for equipment and simpler processes of sample preparation, making them more convenient for testing Hg^{2+}. Usually, these methods can achieve the general detection limit at ~nmol/L. Nevertheless, these methods still cannot meet the needs of high sensitive detection of trace Hg^{2+}, since mercury poisoning is a long-term bioaccumulation related to sub-nmol/L level Hg^{2+}. Furthermore, some optical sensors especially fluorescence are facing the problems of quenching and photo bleaching.

Different from above-mentioned methods, surface-enhanced Raman scattering (SERS) is reported as a novel technology with the advantages of low cost, ultra-sensitivity, high specificity and good signal stability. Detections based on SERS do not require expensive instruments or complex preparation procedures, and the Raman signal acquisition time is as short as a few minutes or even seconds. Recently SERS is seen as a promising tool for qualitative and quantitative detection of various analytes.

To satisfy the urgent demand of detection trace mercury ions, several SERS analytic protocols have been proposed with the superiorities of high sensitivity and selectivity. In recent years, scientists have made great progress in the application of SERS on detecting water-soluble mercury. In that case, some reviews have been reported to mention about SERS-based methods for tracing Hg^{2+} analysis. For instance, Chansuvarn *et al*. [18] wrote a short paragraph at the end of their review to discuss the possibility of SERS for sensing Hg^{2+} by using gold nanoparticles optical sensors. In 2015, Zhan *et al.* [19] reviewed the recent developments on optical sensors for mercury ions in the aspects of colorimetric, fluorescent and SERS assays. However, so far only a few reviews mentioned about SERS-based mercury detections and no one has given a complete summary. Thus, in this review, we present a comprehensive summary relating to the basic principles, detection strategies, recent advances and current challenges of SERS-based Hg^{2+} detections.

2 Concept of SERS

SERS, known as a surface-ultrasensitive vibrational spectroscopic technique, has been studied widely since its discovery in 1973 when Martin Fleischmann observed enhanced Raman signal from pyridine adsorbing on the rough silver electrode [20]. It claims that, when molecules near or on the rough metal surface (i.e. SERS-active substrate), their Raman scattering can be enhanced obviously with an enhancement factor as high as 10^{15}, which allows SERS to detect trace analytes and even single molecule [21,22].

So far, the enhancement mechanisms have been widely studied to explain this extraordinary optical phenomenon. Among various interpretations, two theoretical mechanisms known as long-range electromagnetic theory (EM) and short-range chemical enhancement theory (CE) have been widely accepted.

Electromagnetic field theory is considered as an enhancement of the electromagnetic field on the surface of metallic nanostructures which are excited by the incident light. Briefly, incident light strikes the surface and then polarizes and excites the metal surface free electrons to do collective oscillations (known as surface plasmon resonance (SPR)), generating a dipolar field on the surface. When the incident light and surface plasmon share the resonance frequency, the dipolar field can be coherent with the original excited field, causing localized collective oscillation to redistribute the electric field on surface. Therefore, many strong enhanced electromagnetic fields are formed across the surface, i.e. hot spots. Once a molecule is near or linked to the area within a hot spot, its Raman signal will be greatly enhanced and the signal intensity is proportional to the fourth power of the total enhanced electric field, i.e. $|E|^4$. It is worth to note that if the incident light frequency largely shifts from the SPR frequency of substrate, the enhancement effect can weaken even disappear. In principle, EM enhancement is chemically nonselective and distance-dependent. Specifically, EM enhancement provides the same enhancement for any type of molecules only when these molecules are on or very near the enormous enhanced filed.

However, the electromagnetic theory cannot fully explain the complex magnitude of many SERS phenomena. In that case, CE mechanism was proposed to explain the interaction between chemisorbed molecules and the SERS substrate without the electromagnetic enhancement. The widely accepted chemical enhancement effect is the charge transfer theory. The charge transfer happens between the chemical-absorbed molecule and metal surface, which results in a higher Raman scattering cross section of the molecule than usual [23]. The other assumption is that light of half the energy can be employed to make the HOMO to LUMO transition, when molecule's HOMO and LUMO fall symmetrically about the Fermi level of the metal surface. Hence, the metal surface acts as a charge transfer intermediate, together with adsorbates to produce Raman photons [24,25].

The general findings are that both EM and CE contribute to the final enhancement of Raman signal, and the EM enhancement mainly depends on the nanostructure of the metal surface as well as the distance between molecules and hot spots, while CE enhancement is achieved by changing Ra-

man scattering cross section through the chemical attachment of analyte on substrates. The surface enhancement can provide giant enhancement both in intensity and signal to noise ratio, forming the foundation for the application of SERS as a powerful detection tool.

3 SERS-based mercury ion detections

Recently SERS has been studied widely on detection of mercury ions. According to the enhancement mechanism of SERS, the SERS effect and intensity are strongly dependent on many factors, especially the SERS activity of the substrate, the distance between the signaling molecule (Raman dye) and substrate, as well as the change of molecular structure. Therefore, by changing these factors, two detection modes, signal turn-on and signal turn-off, are mainly employed in the SERS-based assays of mercury ions. For both the detection modes, a Raman dye is added into the detecting system. Signal turn-on mode refers to that when there is no mercury ion in the sample, almost no Raman signal can be detected, and once mercury ions exist in the sample the SERS signal of the Raman dye is obtained and its intensity increases with the raising concentration of mercury ions. On the contrary, the signal turn-off mode refers to that the strongest Raman signal is obtained in the absence of analytes and the signal can be weakened with the increase of mercury ions. In this section, many recently developed approaches of mercury detections based on signal turn-on and turn-off modes are introduced.

3.1 SERS signal turn-on mode

As mentioned above, SERS enhancement can be achieved through several ways. One of the most common methods is to make the Raman dye closer to the SERS substrate. According to the EM mechanism, hot spots are spread on the SERS-active substrate, so when the signal molecules are closer to the substrate, they can experience stronger electromagnetic field to induce higher SERS intensity. The distance between Raman dye and SERS-active substrate can be controlled by special experimental design of the SERS sensor, i.e. the molecule-substrate distance is the largest at the original state and when the mercury ions are added the distance is shortened since the interaction between mercury ions and the sensor. As a result, the Raman dye is closer to the SERS substrate, bringing out a stronger SERS signal.

For example, Sun and co-workers [7] reported a SERS sensor for Hg^{2+} based on the "signal turn-on" strategy (Figure 1(a)). They constructed a SERS-active substrate by using a Si nanowire array (SiNWAr) as a basis first and then decorated AuNPs on the array's surface. Afterward, single stranded DNA-Cy5 tag (ssDNA-Cy5) was dropped onto the SiNWAr@AuNPs substrate in order to fix ssDNA-Cy5 onto the AuNPs through S–Au bond. In principle, since fixed ssDNA-Cy5 is in an open conformation in the liquid, the

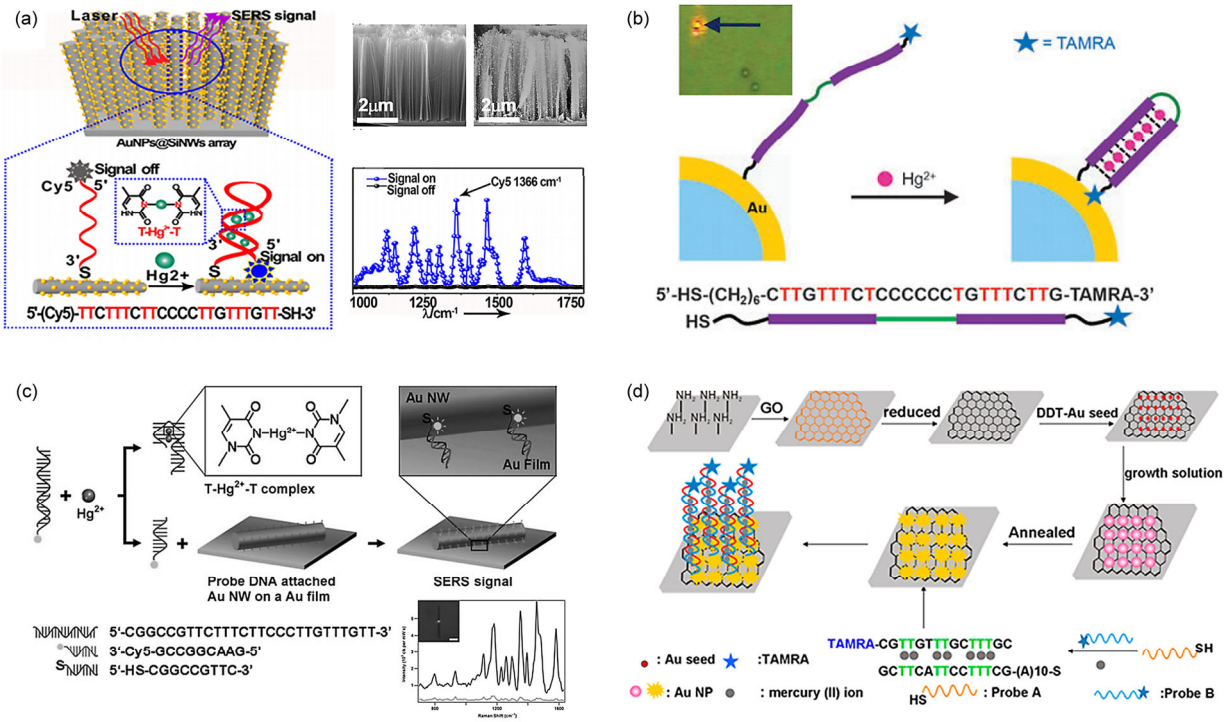

Figure 1 (a) Schematic diagrams of SERS sensor and strategy for Hg^{2+} detection proposed by Sun and coworkers [7]; (b) Schematic diagrams of SERS sensor for Hg^{2+} detection built by Chung's group [26]; (c) SNOF SERRS sensor for Hg^{2+} based on a structure-switching dsDNAs [27]; (d) AuNPs/rGO heterojunction SERS-active substrates and the sensing protocol for Hg^{2+} [28] (color online).

average distance between Cy5 and the SERS substrate is relatively long. However, in the presence of Hg^{2+}, single-stranded DNA structure converted to the hairpin structure with the formation of thymine (T)–Hg^{2+}–T pairs. The hairpin structure pushed Cy5 tag at the 5′ end close to the 3′ end on the AuNPs, which distinctly shortened the distance between Cy5 tag and the SERS substrate. Thus, strong SERS signals were detected, and Hg^{2+} ion with a low concentration of 1 pmol/L was discriminated. Similarly, Chung's group [26] reported an ssDNA-modified gold microshell as a SERS sensor, on which the collected intensity of Raman signal was sensitive to Hg^{2+} concentration (Figure 1(b)). The distance between the gold microshell surface and the Raman tags directly influenced the intensity of SERS signal. In that case, when Hg^{2+} was added, DNA folded into hairpin structure to push tetramethyl-rhodamine (TAMRA) moiety close to the SERS substrate, triggering the generation of SERS signal. The limit of detection (LOD) for Hg^{2+} reached 50 nmol/L.

Besides the formation of a hairpin structure, the exploitation of double stranded DNA (dsDNA) is also able to catch Raman dyes closer to the substrate. Briefly, capture ssDNA is modified on the SERS-active substrate by the 5′ end, while the complementary chain is functioned via linking a Raman dye on the 3′ end. When capture strand matches the complement chain, the dye on the 3′ end will be bond near the capture DNA's 5′ end due to DNA double coiled spiral structure, resulting in a turn-on of SERS signal. For instance, Kang *et al.* [27] demonstrated a DNA3 modified single nanowire-on-film (SNOF) SERS sensor for trace analysis of mercury ions relying on structure switching of double stranded DNAs (Figure 1(c)). If Hg^{2+} did not exist, single stranded T-rich DNA1 could hybridize with the complementary Cy5-labeled DNA2, preventing the hybridization of DNA2 with DNA3 in the next step. Otherwise, the T-rich DNA1 would fold into a hairpin structure through T-Hg^{2+}-T mismatch. Sequentially, it is easy for DNA2 to release from hairpin structural DNA1 and then to combine with probe DNA3. As a consequence, DNA2 carried Raman dyes onto the substrate. The SERS signal turned on and provided a detection limit of 100 pmol/L. Likewise, a T-rich DNA connecting gold nanoparticles (AuNPs)/reduced graphene oxide (rGO) heterojunctions/SiO_2/Si substrate was reported to be a SERS-active substrate for mercury ions detection (Figure 1(d)) [28]. By T-Hg^{2+}-T pairs, T-rich DNA1 coordinated with TAMRA-labeled T-rich DNA2 to form a dsDNA. Since the length of dsDNA was designed within a few nanometers, TAMRA on the DNA2 were fixed very close to the AuNPs, producing strong SERS signal. A very low limit of detection 0.1 nmol/L was implemented from the increasing Raman intensity at 1650 cm^{-1}.

Frequently-used methods for turn-on mode mercury ion detection also include introduction of nanoparticles aggregation. Aggregation is a common way of metallic nanoparticles to generate abundant hot spots at the nanoscale junctions for realizing surface enhancement effect.

In 2011, Lee and Choo [29] reported a SERS-based aptamer sensor for trace analysis of Hg^{2+} in aqueous media (Figure 2). They designed a TAMRA-labelled aptamer probe which could specifically bind to mercury ions. With the help of polyamine spermine tetrahydrochloride, the ssDNA probes absorbed onto the surface of AgNPs, making silver nanoparticles disperse well through enhanced electrostatic repulsion. Once in the presence of Hg^{2+}, the aptamer transformed into a hairpin structure, which caused a reduction of electrostatic repulsion. After that, the aggregation of sliver nanoparticles occurred, resulting in the SERS intensity increasing upon the addition of Hg^{2+}. The limit of detection was 5 nmol/L.

Besides forming aggregates by changing the mutual electrostatic repulsion, scientists also induce the aggregation by constructing sandwich structures between mercury ions and capture molecules absorbed on the SERS-active nanoparticles. Capture molecules can be oligonucleotides containing thymine, cysteine and a variety of small molecules that can chemically bind with mercury ions. Generally, the aggregations induced by the sandwich structure strategy for Hg^{2+} detection are more specific and sensitive. For example, Kuang's group [30] constructed a SERS sensor for mercury ions by assembling gold nanostars (GNS) to dimer structures to obtain SERS-active nanojunctions (Figure 3(A)). The GNS sensor was designed by labeling 4-aminothiophenol (4-ATP) on its surface and then immobilizing T-rich ssDNA1 or complementary ssDNA2 respectively. The Hg^{2+}-mediated T-T base pairs enabled ssDNA1 and ssDNA2 can match with each other to form a dsDNA. The dsDNA acted as linking element, resulting in the GNSs self-assembling into dimers which provided a huge Raman enhancement of the 4-ATP. The limit of detection reached 4 pmol/L and a good linear concentration-intensity relationship from 9.97

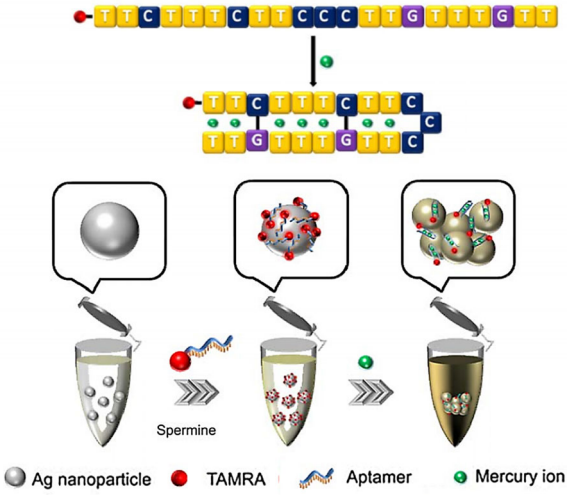

Figure 2 Working principle of the SERS-based Hg^{2+} aptameric sensor. The conformational change of DNA caused the aggregation of silver nanoparticles [29] (color online).

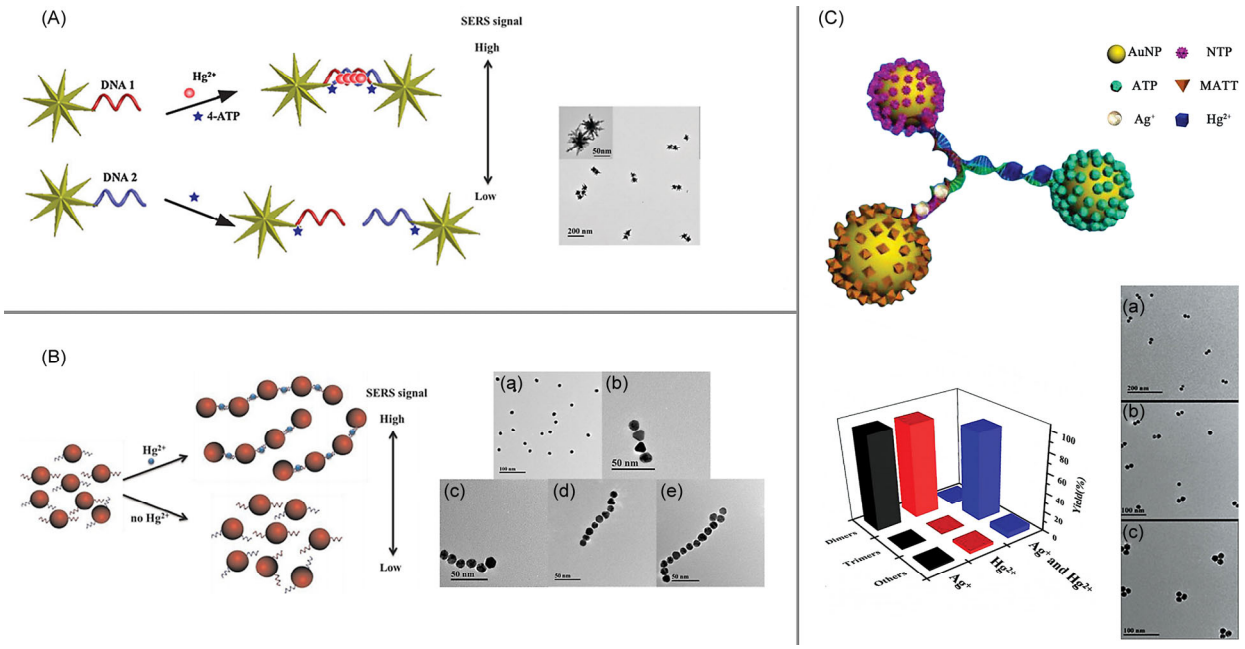

Figure 3 Schematic diagram of the mercury ions detection based on self-assembled AuNPs. (A) GNS dimers [30]; (B) gold assembled nanochains [31]; (C) AuNP trimers [32] (color online).

to 4985 pmol/L was obtained. Moreover, particles also can be assembled into nanochains or trimers structures by controlling the concentration ratio of ssDNA to the nanoparticles. Afterwards, they proposed a protocol for mercury ions detection by assembling gold nanochain constructed by ssDNA modified gold nanoparticles similar to the above-mentioned sensor structure. When adding Hg^{2+}, nanoparticles assembled into chains by the linkage of dsDNA forming T-Hg^{2+}-T base pairs (Figure 3(B)). The length of nanochain was directly proportional to the Hg^{2+} concentration over 0.001–0.5 ng/mL [31]. In the same year, they reported a work on Raman label-encoded gold nanoparticle trimer for detecting Hg^{2+} and Ag^{+} simultaneously (Figure 3(C)) [32]. First, three kinds of ssDNA (DNA 1, 2, 3) were modified to 20 nm AuNPs respectively. Next, AuNP-DNA3 was cultivated with DNA4 and DNA5 which could partially complement DNA3 to structure a "Y-shaped" DNA skeleton. Then, three different AuNP@ DNAs were incubated with three different SERS tags (AuNPs@DNA1@ATP, AuNPs@DNA3-NTP and AuNPs@ DNA2-MATT). When the system contained Hg^{2+} or Ag^{+}, AuNP-DNA1, AuNP-DNA2 and AuNP-DNA3 were assembled into AuNP dimers through the C-Ag^{+}-C or T-Hg^{2+}-T mismatches. Once both Hg^{2+} and Ag^{+} coexisted in the analyte, AuNP trimers were built up, and three characteristic SERS spectra of the three types of Raman reporters were clearly distinguished. The LOD for Ag^{+} and Hg^{2+} simultaneous detection were 8.43 and 8.57 pmol/L, respectively.

Magnetic particles were also used to induce aggregation for mercury ion detection. The corresponding work was devised by Liu *et al.* [33] (Figure 4(a)). Briefly, when Hg^{2+} existed, oligonucleotide modified MSS@Au core/shell NPs (MSS, magnetic silica sphere) could combine to AuNPs@ DNA-DTNB tag (DTNB, 5,5'-dithiobis-(2-nitroben-zoic acid)) through T-Hg^{2+}-T mediated duplex DNA. Then these special structures were effectively collected from surrounding solutions and aggregated by an external magnetic field. They successfully implemented a sensitivity and selectivity detection of trace mercury with LOD at 0.1 nmol/L.

In addition to oligonucleotides, other capture molecules are also applied to induce aggregation, such as cysteine. Wang and co-workers [34] found that cysteine-functionalized Raman dye-labeled silver nanoparticles aggregated in the presence of Hg^{2+} due to the construction of coordination compounds between *L*-cysteine and mercury ions. The experimental results showed an orderly enhanced SERS signal with increasing Hg^{2+} concentration, with an unprecedented LOD of 1 pmol/L. Cecchini *et al.* [35] used the aggregation of AuNPs introduced by polyaromatic ligands (PALs) on a liquid-liquid interface to develop a new mercury detection platform (Figure 4(b)). In their report, an aqueous phase containing AuNPs and Hg^{2+} was placed on top of an organic phase with dissolved PALs. When shaking, the specific interaction between AuNPs and PALs as well as PALs and Hg^{2+} happened at the common phase interface, assembling a network of AuNPs as shown in Figure 4(b). Thus, a SERS signal of PAL was obtained due to the aggregation of AuNPs. The LOD was down to 10 pmol/L. Similar protocol was also mentioned in Shen's work. In their report, polyaniline (PANI) worked as both Raman dye and the mercury ion capture. Both amine and imine groups on PANI can act as adsorption sites of Hg^{2+}. The combination of Hg^{2+} and

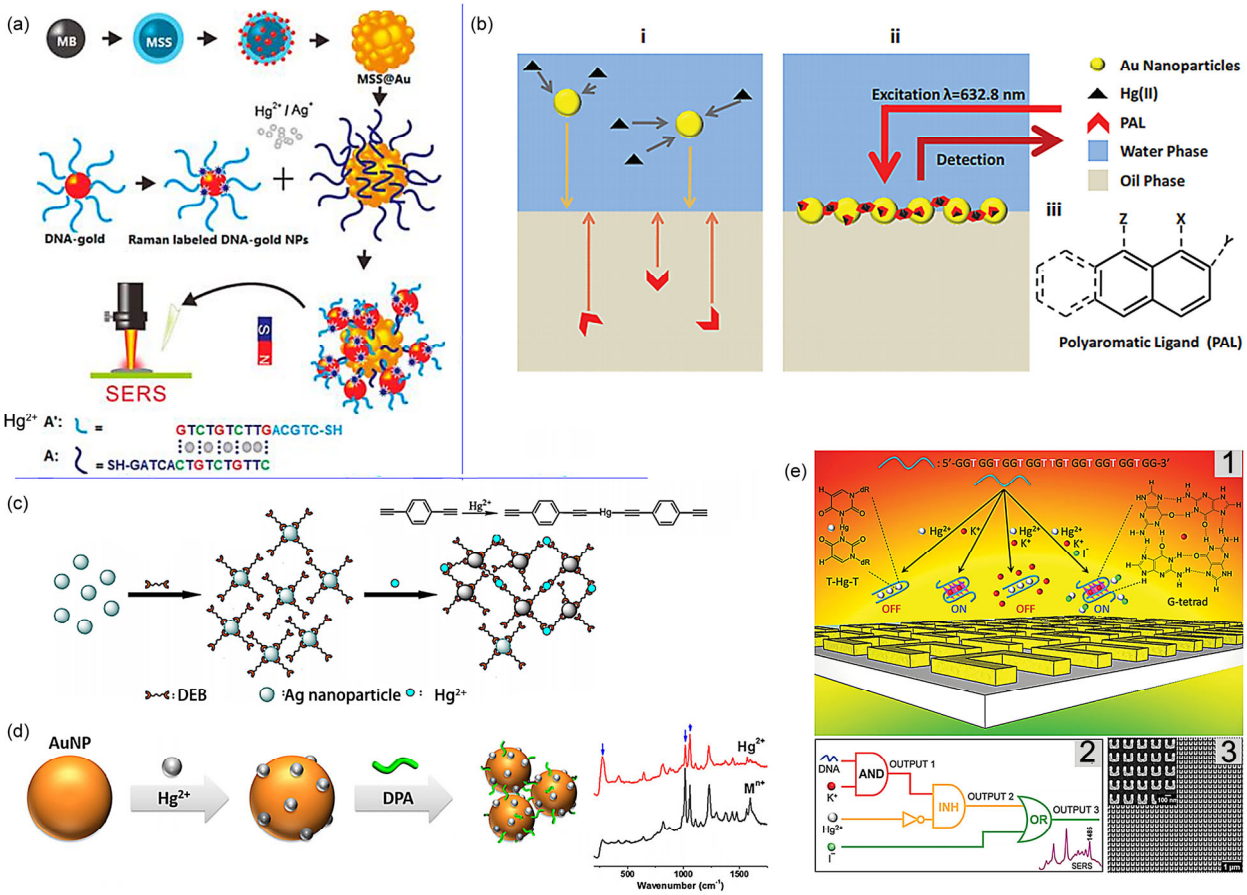

Figure 4 Schematic diagrams of other turn-on mode detections. (a) Hg^{2+}/Ag^{+} detection based on T-Hg-T/C-Ag-C bridges by using DNA-AuNPs and DNA-MSS@AuNPs [33]; (b) Hg^{2+} sensor prepared by using AuNPs and PAL [35]; (c) Hg^{2+} linked to DEB to trigger the aggregation of DEB-labelled AuNPs [38]; (d) detection of Hg^{2+} by means of AuNPs-Hg^{2+}-DPA [43]; (e) combinational logic gate operations (AND, INH, and OR) for mercury ions detection [45] (color online).

PANI weakened the association between PANI and metal surface, reducing the stability of nanoparticles. Alone with the increasing mercury ions concentration, more aggregated nanoparticles appeared, causing peaks such as 1398 and 1560 cm^{-1} a clear SERS enhancement. With the help of Au/PANI composite nanospheres [36] or Ag@PANI core-shell nanoparticles [37], the detection limit of mercury ions was as low as 10 and 1 pmol/L, separately.

Dialkyne 1,4-diethynylbenzene (DEB) not only has the same function as cysteine, but also can work as a Raman dye. Kang and coworkers [38] modified DEB onto the AgNPs first, and then added the Hg^{2+} into colloidal particles (Figure 4(c)). Subsequently, the –C≡C–Hg–C≡C– linkage formed via the interaction between Hg^{2+} and the terminal ethynyl groups of DEB, triggering self-referenced aggregation of AgNPs. As a result, the Raman peak at 2146 cm^{-1} corresponding to Hg–C≡C appears and its intensity was enhanced with the increase of Hg^{2+} concentration, and a detection limit as low as 0.8 nmol/L was obtained.

Compared to the traditional colorimetric method also basing on the aggregation of particles, the LOD can be improved 1000 times for mercury detections by using SERS technique. General colorimetric analyses only reach the concentration limit of Hg^{2+} at ~μmol/L [39–41]. Distinct from colorimetric methods, SERS-based mercury detection methods can discriminate ~nmol/L level and even sub-nmol/L level Hg^{2+} concentration.

Moreover, there are some special materials which can combine with mercury ions causing several changes in their Raman spectral shape. By using these features, several other sensing protocols were proposed. Guerrini *et al.* [42] prepared AuNPs anchored polystyrene microbeads first as SERS substrate and then dropped 4-mercaptopyridine (MPY) onto the beads to form a sensitive SERS sensor for Hg^{2+}. The co-ordination of Hg^{2+} and the nitrogen atom of MPY can normalize the ring breathing of Raman band at 1096 cm^{-1}. In that case, the intensity ratio of the peaks at 799 and 1096 cm^{-1} increased with the raising Hg^{2+} concentration. A low LOD of 250 pmol/L was obtained when the concentration of microbeads was 0.08 μg/mL. Ly and Joo [43] discovered that Hg^{2+} can cause Raman spectral feature changes of di-(2-picolyl)amine (DPA) (Figure 4(d)). If they mixed AuNPs with DPA, the Raman intensity of DPA at 1060 cm^{-1} was weaker than the one at 1020 cm^{-1}. When

they mixed AuNPs with Hg^{2+} first and then added DPA, the previous peak at 1060 cm^{-1} became stronger with the increasing Hg^{2+} concentration, and eventually relative intensities of the 1020 and 1060 cm^{-1} reversed when concentration of Hg^{2+} arrived at about 10 μmol/L.

Turn-on mode detection strategies still utilize some other protocols. For example, mercury ions could be reduced by NaH_2PO_2 to produce nano-mercury which further catalyzed the reduction reaction between NaH_2PO_2 and $HAuCl_4$ to generate AuNPs as SERS-active substrates [44]. Upon the addition of an increasing concentration of Hg^{2+}, more AuNPs were produced to enhance the Raman signal of Vitoria blue B, realizing the LOD of mercury ion down to 0.8 nmol/L.

The coding method operating on a solid SERS substrate was also achieved successfully for Hg^{2+} detection (Figure 4(e)). The thymine- and guanine-rich oligonucleotide sequence has metallophilic abilities to combine Hg^{2+} or K^+, which could specifically interrupt or trigger the formation of Hoogsteen hydrogen bonding. Based on this mechanism, Cao and coworkers [45] demonstrated AND, INHIBIT and OR logic gate operations for sensing metallic ions. When K^+ existing, G-rich oligonucleotides could fold into a specific and stable three-dimensional shape (G-quadruples), in which a distinct Hoogsteen hydrogen-bonded square exhibited a strong Raman signal centered at ~1485 cm^{-1}. Then the following added Hg^{2+} could bind to the thymine to build a hairpin complex, which interrupted the formation of Hoogsteen hydrogen bonding, causing the disappearance of the previous Raman signal. Further, Hg^{2+} can interact with I^+ to form insoluble HgI_2. Thus, further adding I^+, the I^+ removed Hg^{2+} from the oligonucleotide and then the K^+ rebuild G-quadruples, recovering the Raman signal of G-quadruples. They utilized the signal on-off-on change (K^+-Hg^{2+}-I^+) to make AND, INHIBIT and OR logic gates, and the LOD of Hg^{2+} was 1 pmol/L. Table 1 summarizes

Table 1 A summary of different signal turn-on mode SERS sensors for mercury ions

SERS substrate	Raman dye	LOD	Working principle of SERS sensor	Ref.
AuNPs/SiNWAr [a)]	Cy5	0.73 pmol/L	Cy5-labelled-ssDNA [b)] structure converts to the hairpin structure to push Cy5 closer to the SERS substrate	[7]
AuNPs	VBB [c)]	0.8 nmol/L	Hg^{2+} first reduced by NaH_2PO_2 to form nano-mercury that could catalyze the reduction reaction between NaH_2PO_2 and $HAuCl_4$ producing AuNPs	[44]
AuNPs	ATP\MATT\NTP [d)]	12.2 pmol/L	T-Hg^{2+}-T mediated duplex DNA to assemble special dimer or trimer nanostructures	[32]
MSS@Au; AuNPs [e)]	DTNB [f)]	0.1 nmol/L	T-Hg^{2+}-T mediated duplex DNA to combine MSS@AuNPs and AuNPs	[33]
AuNPs	4-NTP	2.24 pmol/L	T-Hg^{2+}-T mediated duplex DNA to trigger the assembling of the DNA modified-AuNPs into nanochains	[31]
AgNPs [g)]	DEB [h)]	0.8 nmol/L	Hg^{2+} linked to DEB to trigger the aggregation of DEB-labelled AgNPs	[38]
Metal SRRs [i)]	G-tetrad	1 pmol/L	AND, INHIBIT and OR logic gate operations based upon the metallophilic properties of a guanine- and thymine-rich oligonucleotide sequence to K^+ and Hg^{2+}	[45]
Au flower particle	PANI [j)]	10 pmol/L	Hg^{2+} bond to nitrogen atoms of PANI on Au flower particle, causing the particle aggregation	[36]
AgNPs	PANI	1 pmol/L	The same principles as above	[37]
Ag@AuNPs	TAMRA [k)]	50 nmol/L	Hg^{2+} introduced transformation of DNA single strain to hairpin structure through T-Hg^{2+}-T pairs to let Cy5 at the end of the ssDNA get closer to the SERS substrate	[26]
AgNPs	TAMRA	5 nmol/L	ssDNA on AgNPs changed into hairpin structure by T-Hg^{2+}-T mismatch, which caused AgNPs aggregation due to the reduced electrostatic repulsion between AgNPs	[29]
Au nanostars	4-ATP	3.99 pmol/L	T-Hg^{2+}-T mediated duplex DNA to assemble special dimer structure of nanostars	[30]
AgNPs	3,5-dimethoxy-4-(6'-azobenzotriazolyl)phenol	1 pmol/L	Hg^{2+} linked to cysteine to trigger the aggregation of cysteine-labelled AuNPs	[34]
Au SNOF [l)]	Cy5	100 pmol/L	T-Hg^{2+}-T pairs induced conformational changes of the ssDNA1 and let DNA1' Raman-labelled complementary match with DNA2 on the SNOF structure	[27]
AgNPs printed film	HgS	N/A	Using a printed film SERS substrate to directly test HgS	[46–48]
AuNPs	PAL [m)]	10 pmol/L	Hg^{2+} linked to PAL to trigger the aggregation of AuNPs	[35]
AuNPs	2MNA [n)]	34 nmol/L	Hg^{2+} affected the intensity ratios of the bands at 1160/1230 cm^{-1} of 2MNA	[49]
AuNPs/rGO/SiO_2/Si [o)]	TAMRA	0.1 nmol/L	T-Hg^{2+}-T pairs induced the formation of dsDNAs and let the Raman reporter get close to the SNOF substrate	[28]

a) AuNPs, gold nanoparticles; SiNWAr, Si nanowire array; b) ssDNA, single-stranded DNA; c) VBB, Vitoria blue B; d) ATP, aminothiophenol; NTP, nitrothiophenol; MATT, 4-methoxy-α-toluenethiol; e) MSS, magnetic silica sphere; f) DTNB, 5,5'-dithiobis-(2-nitrobenzoic acid); g) AgNPs, silver nanoparticles; h) DEB, dialkyne 1,4-diethynylbenzene; i) SRRs, artificial split-ring resonators; j) PANI, polyaniline; k) TAMRA, tetramethyl-rhodamine; l) SNOF, single nanowire-on-film; m) PAL, polyaromantic ligands; n) 2MNA, 2-mercap-toisonicotinic acid; o) rGO, reduced graphene oxide.

the SERS-based mercury ions detections employing signal turn-on mode.

3.2 SERS signal turn-off mode

SERS signal turn-off mode is also a common strategy for mercury ions detection. Usually, the intensity of the Raman signal decreases with the increasing concentration of mercury ions in the analyte. Compared with signal turn-on mode, turn-off mode allows the SERS signal to decay by affecting the Raman dye or the SERS substrate.

A number of Raman dyes can combine with both the SERS substrates and mercury ions, but the Raman dye-binding capacity with mercury ions is stronger than SERS substrates. Therefore, when the mercury ions are present, the dyes preferentially combine with mercury ions, which break the previous absorption between dyes and the SERS substrate, resulting in a decay of dyes' Raman signal.

For instance, Du *et al.* [50] proposed a femtomolar discrimination of mercury ions on an Au@AgNPs modified silicon wafer substrate. 4,4′-dipyridyl (Dpy) was linked to Au@AgNPs via Au–N bond, which can generate a strong Raman signal of Dpy. Once mercury ions were added, Dpy preferentially combined with Hg^{2+} and released from the Ag nanoshells. Since the Dpy molecules were away from the SERS substrate, the SERS signal of Dpy quenched. The LOD was as low as 10 fmol/L. Similarly, R6G molecules were able to combine with Hg^{2+} and then released from AgNPs to decrease their SERS signal. Hereby, Luo *et al.* [51] presented Rhodamine 6G (R6G)-aggregated AgNPs as the sensors to determine Hg^{2+} in the concentration range of 25–2000 nmol/L. Afterwards, Li *et al.* [52] improved the detection protocol by modified R6G with an aminated ring-close structure (R–NH_2) that allowed one Hg^{2+} combined with two R–NH_2 molecules. A more sensitive detection of Hg^{2+} with LOD 1 nmol/L was realized. Tryptophan can also bind to Hg^{2+} to form a 1:2 stable complex and then disassociated from the noble metal. Ray *et al.* [53] reported that tryptophan could coated on the popcorn shaped gold nanoparticles working as both Raman reporter and a protection layer for conserving particles' shaped nanostructure. In the addition of Hg^{2+}, the tryptophan dissociated from the gold nanopopcorns (Figure 5(a)). Moreover, without the protection layer, the previous sharp edges of the nanoparticles dissolved, leading to an attenuation of Raman signal along with the increasing Hg^{2+}. Besides tryptophan, Ma *et al.* [54] prepared the methimazole-functionalized cyclodextrin-protected sliver nanoparticles to be a highly sensitive SERS sensor for mercury ions (Figure 5(b)). The combination of Hg^{2+} with methimazole resulted in desorption of methimazole molecules from the surface of AgNPs, leading to a proportional decreases of SERS signal.

A thrombin-binding aptamer (TBA) can bind to Hg^{2+} or human α-thrombin [55,56], and once the combination

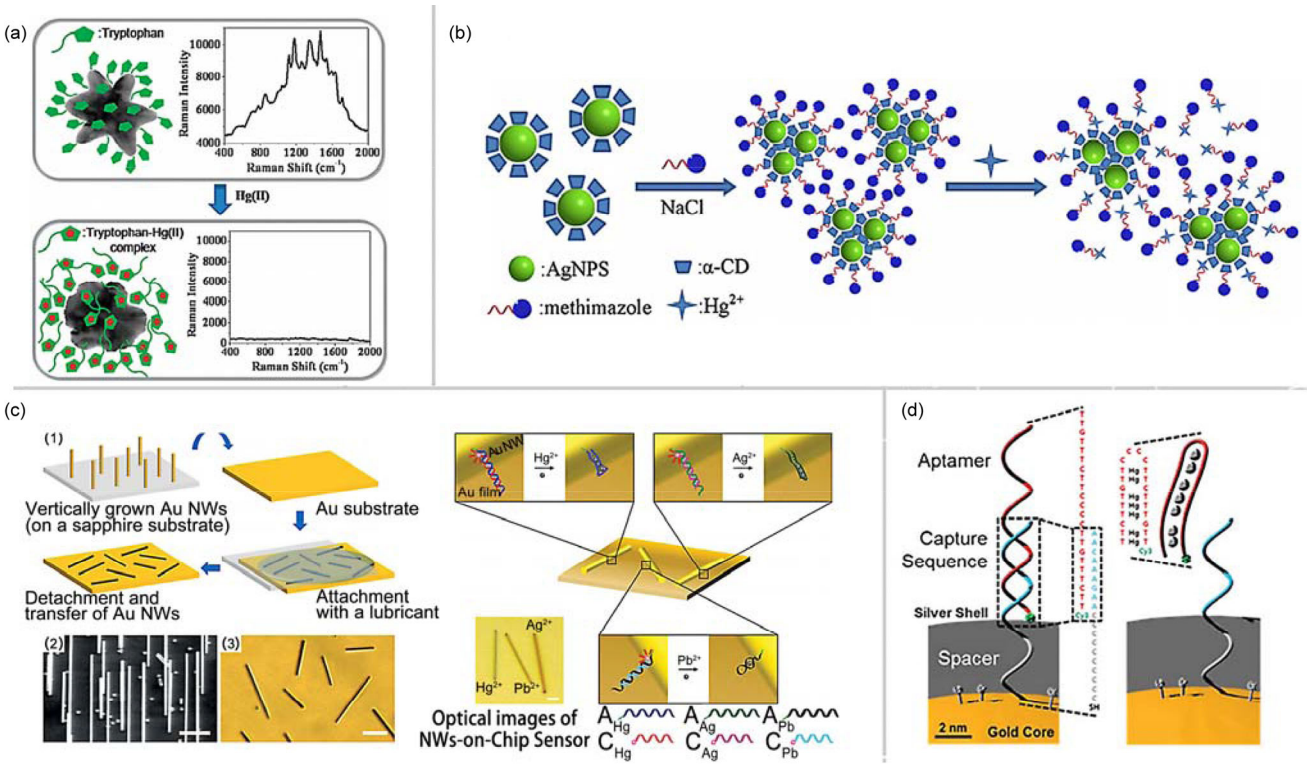

Figure 5 Schematic diagrams of different SERS sensors for Hg^{2+} basing on turn-off mode. (a) Tryptophan protected popcorn shaped gold nanoparticles [53]; (b) methimazole-functionalized cyclodextrin-protected AgNPs [54]; (c) AuNWs/Au substrate [57] and the alignment-addressed AuNWs on-chip SERS sensor [58]; (d) DNA-modified Au@AgNPs [59] (color online).

formed, TBA will dissolve from the metal surface. According to that, a biochemical SERS sensor for analyzing trace Hg^{2+} was fabricated by Kim and co-workers [57]. In their work, they attached Cy5-labeled TBA to the Au nanowires (AuNWs) and then transferred the AuNWs onto an Au film to fabricate a strong SERS-active substrate. With increasing concentration of Hg^{2+} (or human α-thrombin), the SERS signal of Cy5 decreased. In their other report [58], Hg^{2+}, Ag^{+}, and Pb^{2+} were successfully detected simultaneously (Figure 5(c)). They modified ssDNA1 on the AuNWs first and then added Raman dye-modified complementary ssDNA2 to form dsDNA. However, the metallophilic ssDNA2 was easier to bind with specific metal ions than with the complementary chain. Thus, after dropping Hg^{2+} onto the AuNWs, the Raman reporter-labeled ssDNA2 changed into hairpin structure and then were eliminated from the AuNWs, resulting in Raman signal decrease. Three specific metallophilic ssDNA were designed for Hg^{2+}, Ag^{+}, and Pb^{2+} separately and simultaneously used in the experiment for multi ions identification. The LOD were 500 pmol/L, 1 nmol/L, and 50 nmol/L for Hg^{2+}, Ag^{+} and Pb^{2+}, respectively. Similar work was performed by Chung *et al.* [59] and the schematic diagram of detection strategy is shown in Figure 5(d). The SERS signal attenuation showed a good linear relationship with Hg^{2+} concentration from 10 pmol/L to 1 μmol/L.

Of course, that Raman dye escapes from the SERS substrate is not the only method for turn-off mode. Mercury does not have properties to enhance surface Raman. In some cases, mercury ion can be reduced to mercury atoms and then form compounds with gold or silver (i.e. amalgam). The formation of amalgam breaks the original chemical links such as S–Au or S–Ag between Raman dyes and metal surface, removing Raman reporters from the base to cause signal decay. On the other hand, since amalgam integrates with the SERS substrate, it destroys the original nanostructures on metal surface, reducing the Raman enhancement performance of the basis.

Ren and co-workers [60] performed a simple method to form amalgam for sensing the Hg^{2+} in only 2 min via citrate-reduced AgNPs. Citrate on AgNPs reduced Hg^{2+} to Hg^{0} first and then Hg^{0} reacted with AgNPs to form amalgam. Since the amalgam covered on the nanoparticles, both the surface enhancement effect of AgNPs and the adsorption efficiency of Raman reporters decreased. A low concentration of 90.9 pmol/L for Hg^{2+} was recognized. Amalgam could also easily displace R6G from the metal surface. In the other work, R6G linked to AuNPs by electrostatic interaction and escaped from the AuNPs after adding mercury ions [61], resulting a decrease in SERS intensities of R6G. The LOD was as low as 0.5 nmol/L. A more obvious reduction phenomenon was observed by Yang's group (Figure 6(a)) [62]. In their work, inositol hexaphosphate (IP6) stabilized AuNPs were modified by crystal violet (CV as Raman signal molecule) and tri-sodium citrate (TC as reducer) to construct ultrasensitive mercury ion sensors. When mercury ions existing, they were reduced to Hg atoms by TC and absorbed on the AgNPs, as a result the CV molecules were removed from the metal surface. The absorption of Hg atoms onto the AgNPs can be seen from the enlarged diameter of particles in TEM images. An unprecedented LOD of 0.5 pmol/L was obtained. The same experimental principle applies equally to the solid substrate. Kandjani *et al.* [63] promoted a sensing and removal scheme of Hg^{2+} in liquid via a solid SERS-active ZnO/Ag nano-arrays film (Figure 6(b)). ZnO plays two roles here. First, ZnO nano-arrays provided the skeleton for AgNPs to grow; second, as a semiconductor, it offered electrons during the photoreduction process of Hg^{2+} to Hg^{0}. Since Hg^{0} reacted with AgNPs and formed amalgam shells on the AgNPs, the Raman intensity of Rhodamine B (RB) was decayed. The LOD of Hg^{2+} was around 2.25 nmol/L.

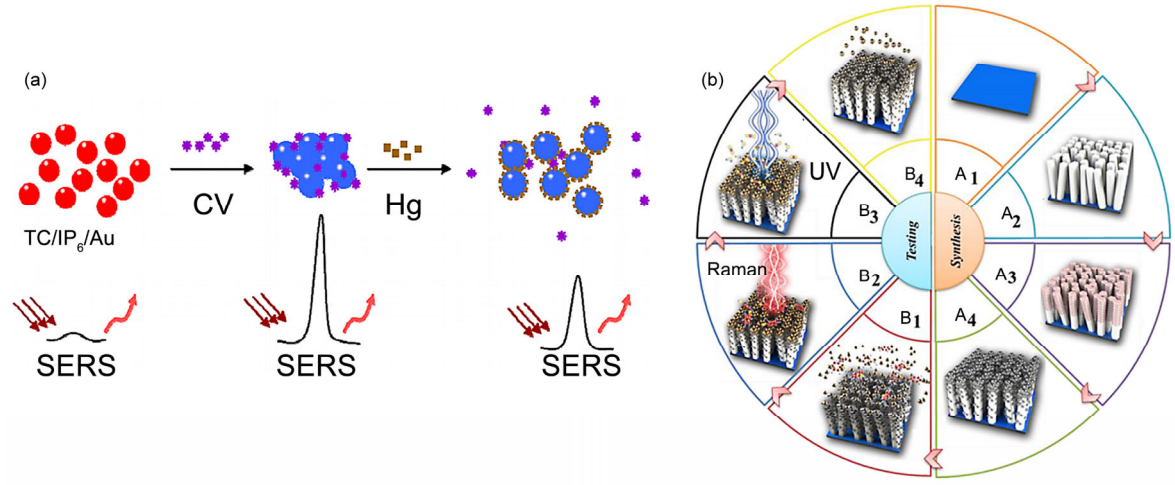

Figure 6 (a) Schematic diagrams of CV/TC/IP_6/AuNPs sensor and working principle [62]; (b) preparation of SERS sensor, sensing mechanism, removal and regeneration processes proposed in Kandjani's work [63] (color online).

In addition, a few other "turn-off" strategies are also available. For instance, Li and co-workers [64] reported a 4-mercaptopyridine (MPy) functioned Ag nanoclusters as SERS sensors for Hg^{2+}. In their work, the MPy protected nanoclusters could stably exist in pH 6.6 buffer solution, with a strong Raman peak of MPy at 1097 cm^{-1}. When mercury ions were added into the colloid, Hg^{2+} could combine with two MPy molecules and cause serious aggregation of Ag nanoclusters precipitating from the solution (Figure 7(a)). The SERS signal at 1097 cm^{-1} dropped as a result of reduced nanoparticles' concentration in the solution.

Zhang *et al.* [65] built a SERS sensor comprises Cy5-labeled thymines-rich ssDNAs and the nanoporous gold film (NPG) (Figure 7(b)). The ssDNAs were consisted of thymines, an –SH at the 5′-terminus and a Cy5 tag at the 3′-end. Through thiol anchors, the ssDNAs were immobilized on the NPG. The ssDNAs tend to lie near the metal surface, out-putting a strong SERS signal of Cy5. When adding Hg^{2+} ions, the ssDNAs formed T-Hg^{2+}-T pairs with each other and transformed into rigid duplex-like complexes that could stand up and push Cy5 away from the SERS substrate, which caused a decrease of SERS signal. By using this SERS sensor, the detection limit as low as 1 pmol/L was obtained. In 2014, a femtogram level SERS-based competitive immunoassay was developed to detect Hg^{2+} in aqueous solution (Figure 7(c)) [66]. Monoclonal antibodies (mAbs) against Hg^{2+} are produced by hybridoma technique. In general, without Hg^{2+}, mAbs can connect to corresponding antigens on the film surface through the combining of the common specific antibodies, known as the sandwich immunoassay. However, Hg^{2+} can react with mAbs but not the corresponding antigens. If mAbs connect with Hg^{2+}, it cannot provide binding sites for corresponding antibodies and let along connect to corresponding antigens on film. In that case, When Hg^{2+} existed, mAbs and 4-mercaptobenzoic acid modified AuNPs had few opportunities to conjugate onto the corresponding antigens-covered substrate, which caused SERS signal decay. The limit of detection reached 0.4 nmol/L. Table 2 summarizes the SERS-based mercury ions detections employing signal turn-off mode.

3.3 SERS based detections combined with other technologies

In recent years, more and more strategies which combine SERS with multiple techniques, such as colorimetry, UV, SPR and fluorescence, have been developed to sense trace mercury ions. These multi-technological detection methods can provide various sensing modes by launching not only SERS but also other optical or electrical signals at the same time. Thereby, it allows the detection results more credible and accurate.

For example, Ma *et al.* [71] demonstrated a SERS and SPR dual-signal mode sensor for mercury ions analysis consisting of PATP-coupled Au nanoparticles' multilayer (Figure 8(a)). The *para*-aminothiophenol (PATP) functioned as coupling molecules between Au nanoparticles to fabricate Au multilayer through layer-by-layer assembly. Nevertheless, PATP's thiol group had a higher binding affinity to Hg^{2+} than Au. Thus, when Hg^{2+} was introduced, Hg^{2+} detached PATP from AuNPs to destroy the multilayer structure, resulting in a response of an intense LSPR extinction band as well as a weaker Raman peak intensity of PATP. The superb selectivity for Hg^{2+} detection reached a low level of 1 nmol/L. Zhan's team [72] designed a colorimetric and SERS dual-signal sensor for Hg^{2+} detection (Figure 8(b)). Bismuthiol II first absorbed onto AuNPs and its extra sulphur atoms had connection ability to other

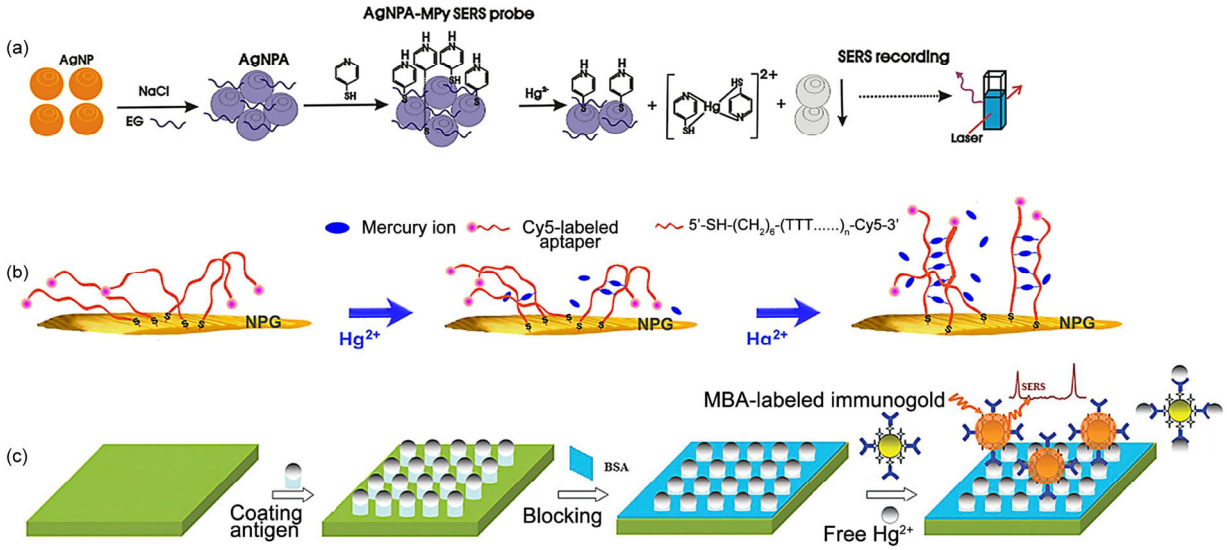

Figure 7 Some SERS sensors and working principles. (a) AgNPA (Ag nanoparticles aggregation)-MPy SERS sensor for Hg^{2+} [64]; (b) SERS sensing of Hg^{2+} based on the aptamer modified NPG [65]; (c) SERS based competitive immunoassay for Hg^{2+} [66] (color online).

Table 2 A summary of different turn-off mode SERS sensors for mercury ions

Substrates	Raman reporters	LOD	Sensing properties	Ref.
Au@AgNPs	Dpy [a)]	10 fmol/L	Dpy coordinated with Hg^{2+} and then released from the SERS substrate	[50]
AgNPs	R6G [b)]	10 nmol/L	SERS intensity decreased owing to the formation of the stable R6G-$HgBr_4^{2-}$ ternary association complex	[51]
Au-Ag alloy NPs	R–NH_2 [c)]	1 nmol/L	Hg^{2+} combined with two R–NH_2 molecules making the R–NH_2 relieved from the SERS substrate	[52]
Popcorn shaped AuNPs	Tryptophan	25 nmol/L	Tryptophan interacted with Hg^{2+} and then being removed from AuNPs	[53]
Cyclodextrin-coated AgNPs	Methimazole	0.5 nmol/L	Desorption of methimazole molecules from the surface of AgNPs due to the present of Hg^{2+}	[54]
AuNWs [d)]	Cy5	10 nmol/L	TBA can bind to Hg^{2+} with a dissociation constant of 25 nmol/L [e)]	[57]
AuNWs	Cy5	500 pmol/L	Hg^{2+} bound to its corresponding aptamer leading a conformational change, thus Raman reporter-attached DNAs released from its complementary aptamers and were eliminated from the AuNW	[58]
Au@AgNPs	Cy3	10 pmol/L	Hg^{2+} bound to its Raman reporter-labeled corresponding aptamer, causing a conformational change of the aptamer and eliminating the ssDNA from the NPs	[59]
AgNPs	CV, BG, EB [f)]	90.9 pmol/L	Hg^{2+} interacted with Ag to form a mercury/Ag shell blocking the adsorption of Raman tag onto Ag surface	[60]
BSA-modified AuNPs [g)]	R6G	0.5 nmol/L	R6G was displaced from the substrate due to the strong affinity between Au and Hg^{2+}	[61]
CV/TC/IP_6/AuNPs [h)]	CV	0.5 pmol/L	Hg atom reduced by TC preferentially absorbed onto AuNPs and replaced the original CV molecules on surface	[62]
ZnO/Ag nanoarrays	RB [i)]	~2.25 nmol/L	Electrons from the ZnO were transferred to the divalent Hg^{2+} to generate Hg atoms which further form amalgam with AgNPs	[63]
AgNPA [j)]	MPy [k)]	30 nmol/L	Stable complex of $[Hg(MPy)_2]^{2+}$ was formed and the AgNPA particles precipitated and released from the solution	[64]
Dealloyed nanoporous gold film	Cy5	1 pmol/L	Hg^{2+} can bind between two DNA thymine bases to reorganize the poly-T oligonucleotides from flexible single strands to relatively rigid duplex-like complexes to push Cy5 away from the SERS substrate	[65]
Immunogold	MBA	0.4 nmol/L	mABs failed to combined with its specific antibody after combined with Hg^{2+}, inhibiting the formation of sandwich structure on Au film	[66]
AuNPs	RB	~2.49 nmol/L	Hg^{2+} can bind to AuNPs preferentially and replace the previous absorbed Raman dyes	[67]
Ag_2TeNPs	R6G	3 nmol/L	Ag_2Te NPs reacted with Hg^{2+} to form HgTe NPs, leading to a decrease of SERS intensity	[68]
AgNPs	4-MPy	0.34 nmol/L	Formed the Hg-Ag alloy and then blocked the adsorption of 4-MPy	[69]
Au@AgNR	MGITC [l)]	1 pmol/L	MGITC can bind strongly with Hg^{2+} to prevent MGITC anchoring onto the substrate	[41]
AuNPs	Diphenylthiocarbazone	1 nmol/L	Hg^{2+} were able to displace the diphenylthiocarbazone molecules from the substrate	[70]

a) Dpy, 4,4′-Dipyridyl; b) R6G, rhodamine 6G; c) R–NH_2, a aminated ring-close structure of rhodamine 6G; d) AuNWs, single crystalline Au nanowires; e) TBA, thrombin-binding aptamer; f) CV, crystal violet; BG, brilliant green; EB, ethidium bromide; g) BSA, bovine serum albumin; h) TC, tri-sodium citrate; IP_6, inositol hexaphosphate; i) RB, rhodamine B; j) NPA, nanosilver-aggregation; k) MPy, 4-mercaptopyridine; l) MGITC, malachite green isothiocyanate.

AuNPs, causing the gold nanoparticle aggregation and producing a strong SERS signal of Bismuthiol II. Then, Hg^{2+} was introduced. Hg^{2+} could bind to sulphur atoms on Bismuthiol II to reduce Bismuthiol II's ability to connect Au. Thus, the aggregation of AuNPs was reversed, leading a quench of Raman signal and a recover at 520 nm of UV spectroscopy. The limit of detection was 2 and 30 nmol/L for UV-Vis spectroscopy and SERS spectroscopy, respectively.

The co-working of fluorescence spectrum and Raman spectrum also becomes popular. A number of fluorescent molecules have a larger Raman scattering cross section which can produce a distinct Raman signal, therefore, the combination experiment of fluorescence and SERS requires only one signal reporter.

For example, Ganbold *et al*. [73] reported a SERS and fluorescence dual-mode ions sensor consisting of citrate-reduced AuNPs covered with rhodamine dyes. Two rhodamine dyes (R6G and Rh123) were introduced in experiment system to be a fluorescent molecule as well as a Raman reporter. In the colloid of rhodamine dyes-covered AuNPs, fluorescent signal quenched and a strong SERS signal of rhodamine was obtained. After Hg^{2+} was put in, rhodamine dyes detached from AuNPs, which weakened fluorescent quenching effect from metal substrate and meanwhile decreased the SERS intensities. To explain rhodamine dyes'

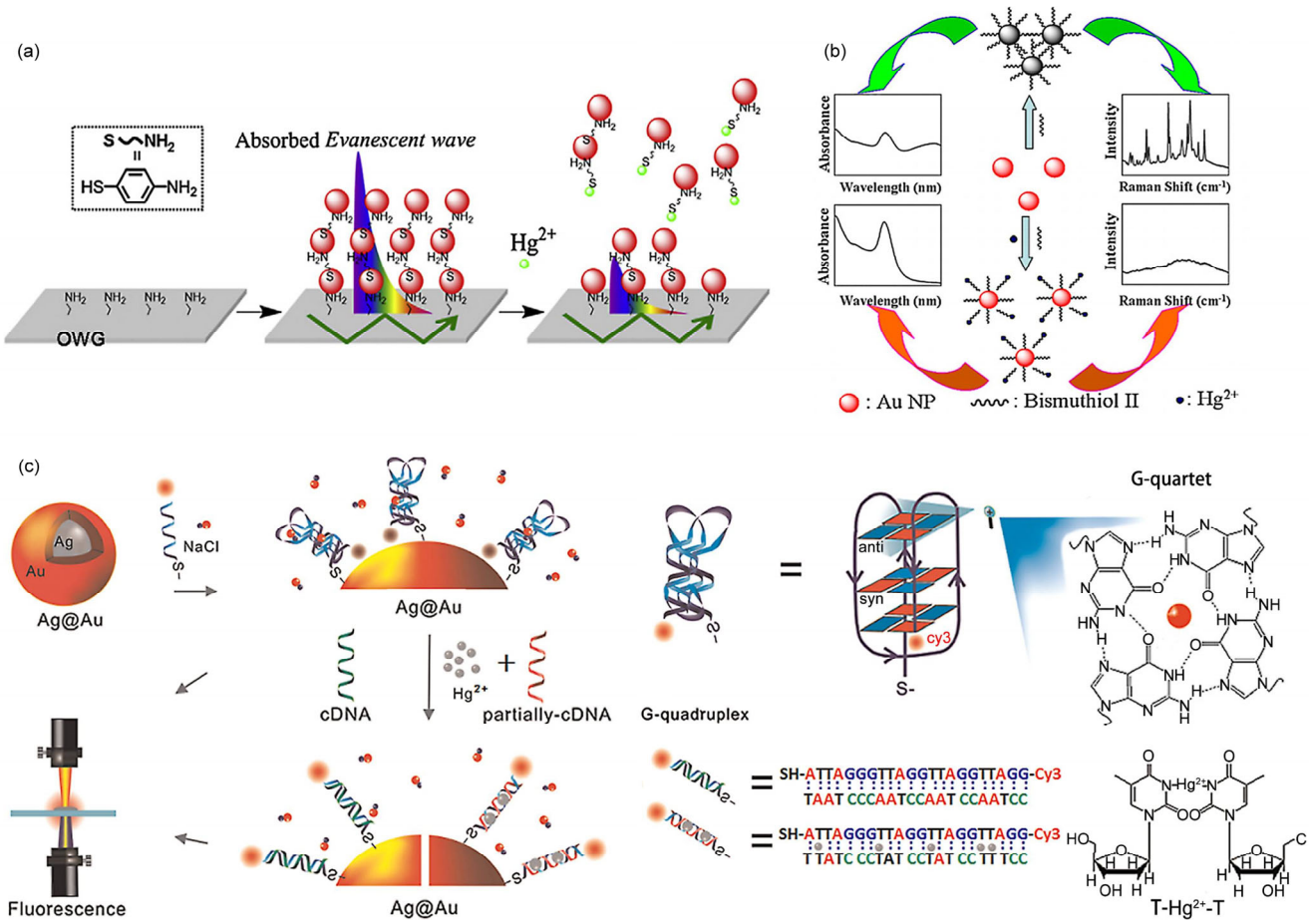

Figure 8 SERS based detections combining with other technologies. (a) SERS and SPR dual-signal model sensor [71]; (b) colorimetric and SERS dual-signal sensor [72]; (c) SERS/fluorescence dual-mode sensor based on the human telomeric G-quadruplex DNA [74] (color online).

detachment, researchers gave two conjectures: rhodamine dyes preferentially bond to Hg^{2+} instead of AuNP surfaces; or mercury ions actually bonds to the AuNPs displacing the rhodamine dyes from the substrate. A dynamic relationship between the mercury ions and the two signals' intensity in the range 0.5–10 μmol/L was observed. Similarly, another SERS/Fluorescence dual-mode nano-sensor for trace mercury was constructed by Liu's group [74] based on the Cy3-linked G-quadruplexes and the Ag@Au nanoparticles (Figure 8(c)). Cy3 was closer to the plasmonic surface when G-quadruplexes was modified on metal surface, generating a strong SERS signal. In addition of complementary DNA and Hg^{2+}, G-quadruplexes was opened up to match with complementary DNA by T-Hg^{2+}-T pairs, leading Cy3 far from the metal surface to restore the fluorescence and decrease the SERS intensity. The LOD was as low as 5 pmol/L.

4 Conclusions

Owing to the serious mercury pollution, developing rapid, ultra-sensitive and reliable methods for detecting mercury ions are now on the agenda and has caused widespread attention. SERS considered as a novel optical technology has great advantages and potentials in sensitive mercury ions detection.

This review summarized the progress on SERS-based mercury ions detections in the past few years. According to the intensity changes of SERS signal, the detection strategies can be primarily divided into two categories, i.e. signal turn-on and turn-off modes. For the turn-on mode, the detection protocols are designed to out-put stronger SERS signals with the increasing mercury ions, mainly by inducing the metallic nanoparticles to form aggregates in order to generate rich hot spots or pushing the Raman dyes closer to the SERS substrate to obtain stronger surface enhancement effect. Turn-off mode primarily utilizes the effects of mercury ions on the dissociation of Raman reporters from the SERS substrate or the forming of amalgam to interfere the surface enhancement effect of the SERS substrates. Besides these two predominant strategies, several combination methods of SERS with other techniques such as fluorescence, UV and SPR were also mentioned and discussed.

SERS has obtained great progress in the detection of mercury ion. However, most protocols based on turn-on mode use noble metal nanoparticles as the SERS-active

substrates which can nonspecifically aggregate due to the influence of environmental factors such as low PH value or high temperature of the ambient environment. Thus, it is important to develop highly stable SERS sensors that can adapt to complexed testing environment. Besides, the stable solid SERS substrates with strong and uniform surface enhancement effect are also required to perform convenient detections with highly repeatable SERS signals. Moreover, since the contaminations always involve multiple toxic heavy metal ions, simultaneous multivariate analysis is an urgent demand. Therefore, developing novel simultaneous detection strategies for multi components testing is also a very important and challenge topic. At present, most applications of SERS for mercury ions detections are still in the laboratory research stage, so the future works also should be focused on bringing the SERS technique to the practical applications.

In summary, SERS technique has shown significant prospects in the field of mercury ions detection, and is hopeful to develop a series of cheap, simple, real-time, *in-situ*, ultrasensitive and reliable detection strategies for practical application in the near future.

Acknowledgments This work was supported by the National Basic Research Program of China (2012CB933301), the National Natural Science Foundation of China (21475064), the Natural Science Foundation of Jiangsu Province of China (BM2012010), the Natural Science Fund for Colleges and Universities in Jiangsu Province (13KJB140009), the Sci-tech Support Plan of Jiangsu Province (BE2014719), the Research Innovation Program for College Graduates of Jiangsu Province (SJZZ15_0107), and the Priority Academic Program Development of Jiangsu Higher Education Institutions (YX03001).

Conflict of interest The authors declare that they have no conflict of interest.

1 Eley BM, Cox SW. *Br Dent J*, 1993, 175: 161–168
2 Nolan EM, Lippard SJ. *Chem Rev*, 2008, 108: 3443–3480
3 Castilhos ZC, Rodrigues-Filho S, Rodrigues APC, Villas-Bôasa RC, Siegel S, Veiga MM, Beinhoff C. *Sci Total Environ*, 2006, 368: 320–325
4 Onyido I, Norris AR, Buncel E. *Chem Rev*, 2004, 104: 5911–5930
5 Palmer R, Blanchard S, Stein Z, Mandell D, Miller C. *Health Place*, 2006, 12: 203–209
6 Harada M. *Teratology*, 1978, 18: 285–288
7 Sun B, Jiang XX, Wang HX, Song B, Zhu Y, Wang H, Su Y, He Y. *Anal Chem*, 2015, 87: 1250–1256
8 Sarica DY, Türker AR. *Clean-Soil Air Water*, 2012, 40: 523–530
9 López-García I, Rivas RE, Hernández-Córdoba M. *Anal Chim Acta*, 2012, 743: 69–74
10 Zhang Y, Li X, Liu G, Wang Z, Kong T, Tang J, Zhang P, Yang W, Li D, Liu L, Xie G, Wang J. *Biol Trace Elem Res*, 2011, 144: 854–864
11 Abdolmohammad-Zadeh H, Jouyban A, Amini R, Sadeghi G. *Microchim Acta*, 2013, 180: 619–626
12 Yu LP, Yan XP. *At Spectrosc*, 2004, 25: 145–153
13 Wu Y, Zhan S, Xu L, Shi W, Xi T, Zhan X, Zhou P. *Chem Commun* 2011, 47: 6027–6029
14 Shah AQ, Kazi TG, Baig JA, Afridi HI, Arain MB. *Food Chem*, 2012, 134: 2345–2349
15 Ye BC, Yin BC. *Angew Chem Int Ed*, 2008, 47: 8386–8389
16 Lou TT, Chen L, Zhang CR, Kang Q, You H, Shen D, Chen L. *Anal Methods*, 2012, 4: 488–491
17 Du J, Liu MY, Lou XH, Zhao T, Wang Z, Xue Y, Zhao J, Xu Y. *Anal Chem*, 2012, 84: 8060–8066
18 Chansuvarn W, Tuntulani T, Imyim A. *TrAC-Trends Anal Chem*, 2014, 65: 83–96
19 Duan JL, Zhan JH. *Sci China Mater*, 2015, 58: 223–240
20 Fleischmann M, Hendra PJ, Mcquillan AJ. *Chem Phys Lett*, 1974, 26: 163–166
21 Kneipp K, Wang Y, Kneipp H, Perelman LT, Itzkan I, Dasari RR, Feld MS. *Phys Rev Lett*, 1997, 78: 1667–1670
22 Nie SM, Emory SR. *Scinece*, 1997, 275: 1102–1106
23 Kneipp K, Kneipp H, Itzkan I, Dasari RR, Feld MS. *Chem Rev*, 1999, 99: 2957–2976
24 Campion A, Kambhampati P. *Chem Soc Rev*, 1998, 27: 241–250
25 Michaels AM, Brus L. *J Phys Chem B*, 2000, 104: 11965–11971
26 Han D, Lim SY, Kim BJ, Piao L, Chung TD. *Chem Commun*, 2010, 46: 5587–5589
27 Kang T, Yoo SM, Yoon I, Lee S, Choo J, Lee SY, Kim B. *Chem-Eur J*, 2011, 17: 2211–2214
28 Ding XF, Kong LT, Wang J, Fang F, Li DD, Liu JH. *ACS Appl Mater Interfaces*, 2013, 5: 7072–7078
29 Lee C, Choo J. *Bull Korean Chem Soc*, 2011, 32: 2003–2007
30 Ma W, Sun MZ, Xu LG, Wang L, Kuang H, Xu C. *Chem Commun*, 2013, 49: 4989–4991
31 Xu LG, Yin HH, Ma W, Kuang H, Wang L, Xu C. *Biosens Bioelectron*, 2014, 67: 472–476
32 Li S, Xu LG, Ma W, Kuang H, Wang L, Xu C. *Small*, 2015, 11: 3435–3439
33 Liu M, Wang ZY, Zong SF, Chen H, Zhu D, Wu L, Hu G, Cui Y. *ACS Appl Mater. Interf*, 2014, 6: 7371–7379
34 Lia F, Wanga J, Laia Y, Wua C, Sunb S, Heb Y, Mab H. *Biosens Bioelectron*, 2013, 39: 82–87
35 Cecchini MP, Turek VA, Demetriadou A, Britovsek G, Welton T, Kornyshev AA, Wilton-Ely JDET, Edel JB. *Adv Opt Mater*, 2014, 2: 966–977
36 Wang XF, Shen YH, Xie AJ, Li SK, Cai Y, Wang Y, Shu HY. *Biosens Bioelectron*, 2011, 26: 3063–3067
37 Wang XF, Shen YH, Xie AJ, Chen SH. *Mater Chem Phys*, 2013, 140: 487–492
38 Kang Y, Wu T, Liu BX, Wang X, Du Y. *Microchim Acta*, 2014, 181: 1333–1339
39 Bothra S, Solanki JN, Sahoo SK. *Sensor Actuat B-Chem*, 2013, 188: 937–943
40 Chai F, Wang C, Wang TT, Ma ZF, Su ZM. *Nanotechnology*, 2010, 21: 862–865
41 Chen SH, Liu DB, Wang ZH, Sun X, Cui D, Chen X. *Nanoscale*, 2013, 5: 6731–6735
42 Guerrini L, Rodriguez-Loureiro I, Correa-Duarte MA, Lee YH, Ling XY, Javier Garcia De Abajo F, Alvarez-Puebla RA. *Nanoscale*, 2014, 6: 8368–8375
43 Ly NH, Joo S. *Bull Korean Chem Soc*, 2015, 36: 226–229
44 Liang AH, Shang GY, Ye LL, Wen G, Luo Y, Liu Q, Zhang X, Jiang Z. *RSC Adv*, 2015, 5: 21326–21331
45 Cao C, Zhang J, Li SZ, Xiong QH. *Small*, 2014, 10: 3252–3256
46 Eshkeiti A, Reddy ASG, Narakathu BB, Joyce MK, Bazuin BJ, Atashbar MZ. *IEEE Sensor*, 2012: 434–437
47 Eshkeiti A, Narakathu BB, Reddy ASG, Moorthi A, Atashbar MZ, Rebrosova E, Rebros M, Joyce M. *Sensor Actuat B-Chem*, 2012, 171: 705–711
48 Eshkeiti A, Narakathu BB, Reddy ASG, Moorthi A, Atashbar MZ. *Procedia Eng*, 2011, 25: 338–341
49 Tan EZ, Yin PG, Lang XF, Zhang HY, Guo L. *Spectro Acta Pt A-Molec Biomolec Spectr*, 2012, 97: 1007–1012
50 Du YX, Liu RY, Liu BH, Wang SH, Han MY, Zhang Z. *Anal Chem*, 2013, 85: 3160–3165

51 Luo YH, Li K, Wen GQ, Liu Q, Liang A, Jiang Z. *Plasmonics*, 2012, 7: 461–468
52 Li P, Liu HL, Yang LB, Liu J. *Talanta*, 2013, 106: 381–387
53 Senapati T, Senapati D, Singh AK, Fan Z, Kanchanapally R, Ray PC. *Chem Commun*, 2011, 47: 10326–10328
54 Ma PY, Liang FH, Yang QQ, Wang D, Sun Y, Wang XH, Gao D, Song D. *Microchim Acta*, 2014, 181: 975–981
55 Cho H, Baker B, Wachsmann-Hogiu S, Pagba CV, Laurence T, Lane S, Lee LP, Tok BH. *Nano Lett*, 2008, 8: 4386–4390
56 Liu CW, Huang CC, Chang HT. *Anal Chem*, 2009, 81: 2383–2387
57 Kim H, Kang T, Lee H, Ryoo H, Yoo SM, Lee SY, Kim B. *Chem-Asian J*, 2013, 8: 3010–3014
58 Kang T, Yoo SM, Kang M, Lee H, Kim H, Lee SY, Kim B. *Lab Chip*, 2012, 12: 3077–3081
59 Chung E, Gao R, Ko J, Choi N, Lim DW, Lee EK, Chang SI, Choo J. *Lab Chip*, 2012, 13: 260–266
60 Ren W, Zhu CZ, Wang EK. *Nanoscale*, 2012, 4: 5902–5909
61 Ji W, Chen L, Xue XX, Guo ZN, Yu Z, Zhao B, Ozaki Y. *Chem Commun*, 2013, 49: 7334–7336
62 Fu SY, Guo XY, Wang H, Yang TX, Wen Y, Yang HF. *Sensor Actuat B-Chem*, 2014, 199: 108–114
63 Kandjani AE, Sabri YM, Mohammad-Taheri M, Bansal V, Bhargava SK. *Environ Sci Technol*, 2015, 49: 1578–1584
64 Li K, Liang AH, Jiang CN, Li F, Liu Q, Jiang Z. *Talanta*, 2012, 99: 890–896
65 Zhang L, Chang H, Hirata A, Wu H, Xue QK, Chen M. *ACS Nano*, 2013, 7: 4595–4600
66 Wang YZ, Chen S, Wei C, Xu MM, Yao JL, Li Y, Deng A, Gu R. *Chem Commun*, 2014, 50: 9112– 9114
67 Wang G, Lim C, Chen L, Chon H, Choo J, Hong J, Demello AJ. *Anal Bioanal Chem*, 2009, 394: 1827–1832
68 Wang CW, Lin ZH, Roy P, Chang HT. *Front Chem*, 2013, 1: 20
69 Chen LX, Qi N, Wang XK, Chen L, You H, Li J. *RSC Adv*, 2014, 4: 15055–15060
70 Grasseschi D, Zamarion VM, Araki K, Toma HE. *Anal Chem*, 2010, 82: 9146–9149
71 Ma YM, Liu HL, Qian K, Yang LB, Liu JH. *J Colloid Interf Sci*, 2012, 386: 451–455
72 Duan JL, Yang M, Lai YC, Yuan JP, Zhan JH. *Anal Chim Acta*, 2012, 723: 88–93
73 Ganbold EO, Park JH, Ock KS, Joo SW. *Bull Korean Chem Soc*, 2011, 32: 519–523
74 Liu M, Wang ZY, Pan LQ, Cui YP, Liu YM. *Biosens Bioelectron*, 2015, 69: 142–147